

Epitaxial Layer Design for High Performance GaAs pHEMT SPDT MMIC Switches

Jung-Hun Oh, Jae Kyoung Mun, Jin-Koo Rhee, and Sam-Dong Kim

ABSTRACT—From a hydrodynamic device simulation for the pseudomorphic high electron mobility transistors (pHEMTs), we observe an increase of maximum extrinsic transconductance and a decrease of source-drain capacitances. This gives rise to an enhancement of the switching speed and isolation characteristics as the upper-to-lower planar-doping ratios (UTLPDR) increase. On the basis of simulation results, we fabricate single-pole-double-throw transmitter/receiver monolithic microwave integrated circuit (MMIC) switches with the pHEMTs of two different UTLPDRs (4:1 and 1:2). The MMIC switch with a 4:1 UTLPDR shows about 2.9 dB higher isolation and approximately 2.5 times faster switching speed than those with a 1:2 UTLPDR.

Keywords—pHEMT, hydrodynamic device simulation, upper-to-lower planar-doping ratio, SPDT MMIC switch, isolation, switching speed.

I. Introduction

As modern digital systems become highly sophisticated, switches are emerging as key elements significantly determining the overall terminal performance [1]. Methods to improve or optimize the characteristics of the switch ICs can be categorized into two types. One type deals with the circuit configurations, and the other manipulates the core devices, such as pseudomorphic high electron mobility transistors (pHEMTs). There is a limitation in improving the performance of the switch ICs only by dealing with the circuit configuration. Therefore, it is essential to perform analytic research especially

on the pHEMT epitaxial-layer design to enhance the transistor-level switching performance.

In this study, we examine the effects of the doping concentration ratio between the upper and lower planar-doping layers on the electrical characteristics of the double planar-doped pHEMTs for switching applications. Hydrodynamic simulations were first performed, and two types of pHEMT doping structures were then selected for a comparative study. Using the pHEMT structures of two different doping ratios, we fabricated single-pole-double-throw (SPDT) transmitter/receiver (Tx/Rx) monolithic microwave integrated circuit (MMIC) switches.

II. Optimization of the Epitaxial Layer Structure

To examine the pHEMT characteristics depending upon the upper-to-lower planar-doping ratio (UTLPDR), we performed the hydrodynamic model device simulations installed in ISE-TCAD tool of Synopsys [2]. In performing the simulations, the same conditions were maintained except the planar-doping ratios and gate recess depths. The planar-doping ratios were split into 8 conditions as summarized in Table 1. The epitaxial structures used in this study were same as in [3]. The etch-stop current in the gate recess process was controlled to achieve the same drain saturation current (I_{dss}) regardless of the UTLPDR in the simulation. This is why the I_{dss} is reciprocally proportional to the on-state resistance (R_{on}) of the pHEMT switch.

Insertion loss (IL), isolation, and switching speed are the most important parameters determining the switching performance of field effect transistors. The effects of the doping ratio on these parameters can be estimated from the simulation results. Since the I_{dss} was controlled to the same value above

Manuscript received Oct. 30, 2008; revised Feb. 25, 2009; accepted Apr. 13, 2009.

This work was supported by the Millimeter-wave Innovation Technology Center (MINT) at Dongguk University, Seoul, and ETRI, Daejeon, Rep. of Korea.

Jung-Hun Oh (phone: + 82 2 2260 8836, email: newuss@dgu.edu), Jin-Koo Rhee (email: jkrhee@dgu.edu), and Sam-Dong Kim (email: samdong@dgu.edu) are with the Department of Electronic Engineering, Dongguk University, Seoul, Rep. of Korea.

Jae Kyoung Mun (phone: + 82 42 860 6252, email: jkmun@etri.re.kr) is with the Convergence Components & Materials Research Laboratory, ETRI, Daejeon, Rep. of Korea.

Table 1. Summary of various UTLPDRs used for the simulations.

No. of sample	1	2	3	4	5	6	7	8
Upper planar doping ($\times 10^{12}/\text{cm}^2$)	1.0	1.8	2.75	3.7	4.1	4.4	4.5	4.7
Lower planar doping ($\times 10^{12}/\text{cm}^2$)	4.5	3.7	2.75	1.8	1.4	1.1	1.0	0.8
Planar doping ratio (upper : lower)	1:4.5	1:2	1:1	2:1	3:1	4:1	4.5:1	6:1

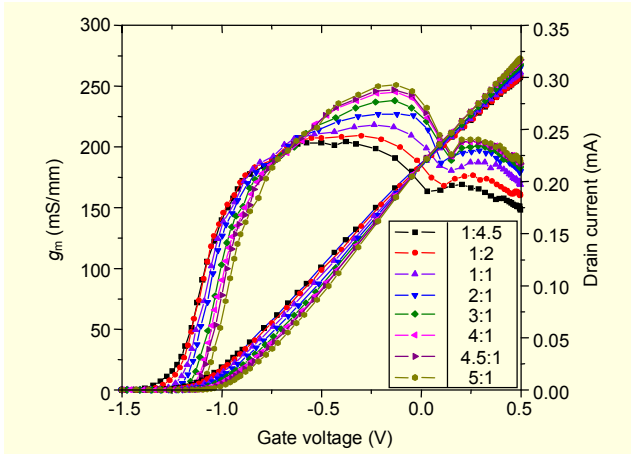


Fig. 1. Calculated I_{ds} versus V_{gs} and g_m characteristics at V_{ds} of 3 V and various UTLPDRs.

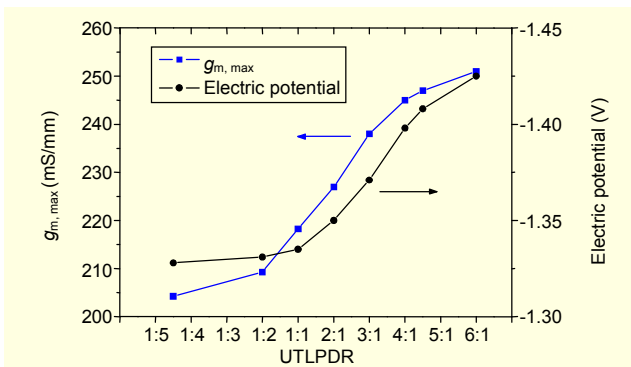


Fig. 2. Electric potential of the InGaAs channel region (at V_{gs} of -3 V and V_{ds} of 0 V) and maximum g_m (at V_{ds} of 3 V and V_{gs} of -0.25 V) versus UTLPDR.

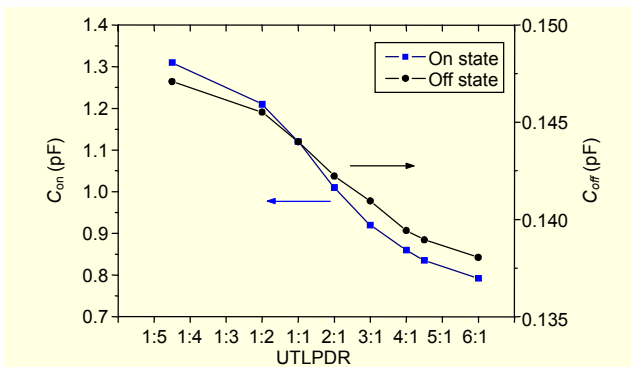


Fig. 3. Calculated C_{on} and C_{off} versus UTLPDR.

V_{ds} of 2 V at any V_{gs} and UTLPDR, the R_{on} was also almost the same regardless of the UTLPDR. The IL is directly proportional to the R_{on} , and this reveals that the IL has negligible dependence on the UTLPDR. Figure 1 shows the calculated drain current (I_{ds}) versus V_{gs} and extrinsic transconductance (g_m) characteristics at various UTLPDRs.

Figure 2 shows the calculated electric potential in the InGaAs channel region and maximum g_m ($g_{m,max}$) at various UTLPDRs. The electric potential negatively increases with the increase of UTLPDR, and this means that the electron density in the channel and the off-state source-to-drain leakage current all decrease with the increase of UTLPDR. As shown in Fig. 3, the on-state source-to-drain capacitance (C_{on}) and the off-state source-to-drain capacitance (C_{off}) decrease with the increase of UTLPDR. Because the isolation characteristic is enhanced with the decrease of C_{off} and the off-state leakage current, a superior isolation characteristic can be expected from the HEMT structure of a higher UTLPDR [4], [5].

Switching speed depends on both g_m and CR-time, where the CR-time is defined as a product of junction capacitance and series resistance [6]. As previously mentioned, channel resistance is not a function of UTLPDR. This means the gate capacitance alone will determine the CR-time.

Figure 3 shows that both C_{on} and C_{off} decrease with the increase of UTLPDR; therefore, the CR-time is reduced with the increase of UTLPDR. As shown in Fig. 2, a higher maximum g_m ($g_{m,max}$) also contributes to enhanced switching speed at a higher UTLPDR. Note that $g_{m,max}$, C_{on} , and C_{off} are all saturated above a UTLPDR of 4:1 as shown in Figs. 2 and 3. Therefore, the upper planar-doping concentration should be at least four times greater than the lower planar-doping concentration for a high performance pHEMT switch in terms of switching speed and isolation.

III. Characteristics of SPDT Tx/Rx MMIC Switches

Based on the simulation results, two types of pHEMTs (UTLPDRs of 4:1 and 1:2) were selected to fabricate the MMIC switches. The measured DC characteristics and extracted C_{on} and C_{off} from the fabricated pHEMTs were in good agreement with the calculations. The 0.5 μm GaAs process of ETRI [3], [7] was used to fabricate the SPDT Tx/Rx

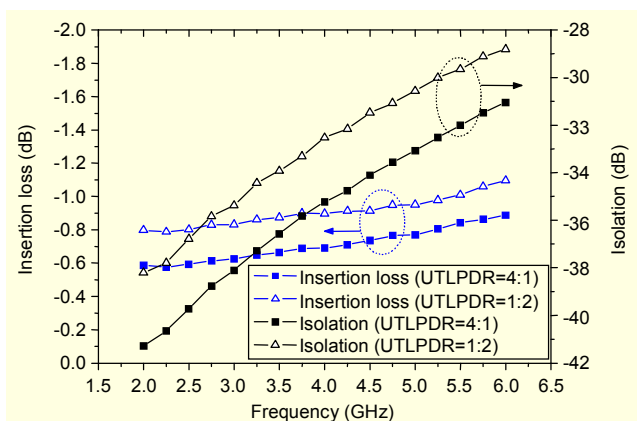


Fig. 4. Measured IL and isolation characteristics for two types of SPDT MMIC switches.

Table 2. Comparison of electrical characteristics of SPDT MMIC stitches based on the pHEMT at 2.4 GHz

Company	Insertion loss (dB)	Isolation (dB)
M/A-COM	-0.65	-25
SkyWorks	-0.55	-23
TriQuint	-0.60	-28
This work	-0.58	-40.2

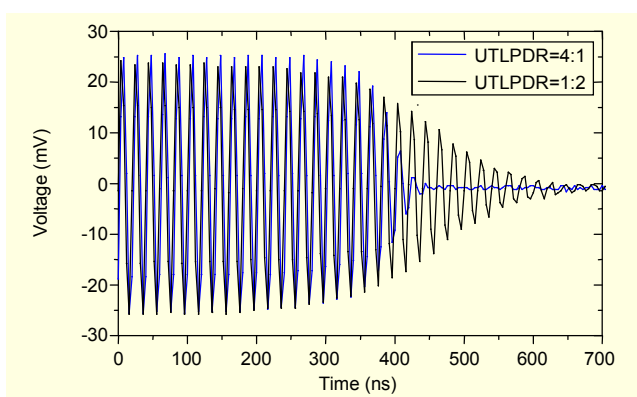


Fig. 5. Measured falling times for two types of SPDT MMIC switches.

MMIC switches. For the circuit design of the SPDT MMIC switches, we used a switch transistor with a 400 μm gate periphery for each path and a shunt-series circuit configuration that is widely used in 2.4 GHz and 5.8 GHz wireless local area network system applications.

As shown in Fig. 4, the MMIC switch of a 4:1 UTLPDR showed about 2.9 dB higher isolation than that of a 1:2 UTLPDR over the entire measurement frequency range of 2 GHz to 6 GHz, while there was only about 0.2 dB difference in IL. This performance enhancement in terms of isolation showed good agreement with the prediction given by the

device simulation. As shown in Table 2, the measured IL and isolation characteristics with a UTLPDR of 4:1 were comparable or even superior to those of commercial chips. We measured the switching speeds at 2.4 GHz by applying a 100 kHz 50% duty pulse signal to the gate control electrodes of the SPDT switches. At -2/0 V control voltages, the falling times were measured, and these are plotted in Fig. 5. These were about 100 ns and 250 ns at 4:1 and 1:2 UTLPDRs, respectively.

The power characteristics were measured at a frequency of 2.4 GHz. The SPDT switch with UTLPDRs of 4:1 and 1:2 shows the output 1 dB compression points of 27 dBm and 25 dBm, respectively, and IP3 values of 42.2 dBm and 43.2 dBm, respectively.

IV. Conclusion

Higher isolation and switching speed were expected above a UTLPDR of 4:1 in the hydrodynamic pHEMT simulation. The SPDT Tx/Rx MMIC switch fabricated with pHEMTs with a 4:1 UTLPDR showed about 2.9 dB higher isolation and 2.5 times faster switching speed than with a 1:2 UTLPDR. Based on the simulation and measurements, we propose that the UTLPDR must be greater than 4:1 for the best switching performance.

References

- [1] J. Kim et al., "A High-Performance 40-85 GHz MMIC SPDT Switch Using FET-Integrated Transmission Line Structure," *IEEE Microw. Wireless Compon. Lett.*, vol. 13, no. 12, 2003, pp. 505-507.
- [2] J.-H. Oh et al., "Effects of Gate-Recess Structure on High-Frequency Characteristics of 0.1 μm Metamorphic HEMTs," *J. Electrochem. Soc.*, vol. 154, no. 7, 2005, pp. G266-G270.
- [3] J.K. Mun et al., "Design and Fabrication of pHEMT MMIC Switches for IEEE 802.11.a/b/g WLAN Applications," *Semiconductor Science and Technology*, vol. 20, pp. 677-84.
- [4] K.-Y. Lin et al., "Millimeter-Wave MMIC Single-Pole-Double-Throw Passive HEMT Switches Using Impedance-Transformation Networks," *IEEE Trans. Microw. Theory Tech.*, vol. 51, no. 4, 2003, pp. 1076-1085.
- [5] Y. Chung et al., "Characterization of Source-to-Drain Capacitance Effect of GaAs pHEMT for Microwave and Millimeter-Wave Switch," *IEEE MTT-S Int. Microw. Symp. Digest*, 2000, pp. 173-176.
- [6] M. Kurata, "Design Considerations of Step Recovery Diodes with the Aid of Numerical Large-Signal Analysis," *IEEE Trans. Electron Devices*, vol. 19, no. 11, 1972, pp. 1207-1215.
- [7] J.-W. Lim et al., "A Comparative Study of a Dielectric-Defined Process on AlGaAs/InGaAs/GaAs pHEMTs," *ETRI Journal*, vol. 27, no. 3, 2005, pp. 304-311.